

Free surface instability in a confined suspension jet

Alejandra Alvarez^{1,2}, Eric Clement³ and Rodrigo Soto^{1,4*}

¹ *Departamento de Física, FCFM, Universidad de Chile, Casilla 487-3, Santiago, Chile.*

² *Instituto de Innovación en Minería y Metalurgia, IM2, avda. del Valle 738, Huechuraba, Santiago, Chile.*

³ *L.M.D.H. - PMMH ESPCI. 10, rue Vauquelin. 75231 Paris Cedex 05, France*

⁴ *Departamento de Física Aplicada I (Termología), Facultad de Ciencias Físicas, Universidad Complutense, 28040 Madrid, Spain*

(Dated: July 18, 2021)

A jet of non-Brownian particles confined in a thin cell and driven by gravitational force is studied both numerically and theoretically. We present a theoretical scheme aimed to describe such a system in the Stokes regime. We focus on the dynamics of the interface between the suspension and the pure fluid. Numerical simulations solving Newton's equations for all particles show that the jet free surface becomes unstable: the fastest growing modes at small sizes coarsen up to the largest structures reaching the jet lateral scale. In the bulk, structural waves develop and travel at slightly slower speed than the jet average fall. An analytical model, based on hydrodynamic-like equations for the suspension, is derived and predicts the development of the interfacial instability. It captures in essence, the collective effects driving the interface destabilization i.e. the long range hydrodynamic interactions coupled with the abrupt interface, and no analogous to a surface tension is found.

PACS numbers: 47.15.Pn, 47.55.Kf, 83.80.Hj

I. INTRODUCTION

Understanding the dynamics of 3D non-Brownian suspension in the low Reynolds number regime is a long lasting and difficult issue. Long-range hydrodynamics forces create a complex collective particle dynamics^{1,2} and up to now, no rigorous closed-form formulation of the problem exists at moderate densities. For example, difficulties remains such as to explain particle sedimentation, dispersion and mixing in a finite size container (see³ and references inside). Recently, the miniaturization of hydrodynamics devices^{4,5}, necessary to develop microfluidic apparatus performing at low Reynolds number, mixing or separation, has brought to the front the importance of boundary confinement of suspensions. In fact, numerous devices bear the form of narrow channels or Hele-Shaw cells with one direction reaching only few particle sizes⁶. Note that experimentally quasi-2D non-Brownian suspensions have also been studied in the case where the cell gap was almost the particle size^{7,8,9}. In this case, the existence of anti-drag correlations due to fluid recirculation around each grains were identified⁹.

To get a better description of mixing, an important basic issue is to capture the evolution of an interface between a suspension and a particle-free fluid (the pure fluid). This problem is also related to many studies done to understand miscible interfaces dynamics, either from two different fluids¹⁰ or a fluid in contact with a suspension falling under gravity^{11,12,13}.

Here, we describe the evolution of a jet of suspended particles in a thin cell driven by gravitational forces. The suspension is non Brownian and the hydrodynamic forces between particles are obtained in the Stokes regime. Numerical simulations that solve the Newton equations for all particles follow the evolution of the jet free surfaces. We present an analytical model, based on hydrodynamic-like equations for the suspension which is able to predict the development of the instability. We present and extend a scheme that was developed recently, in the context of a 2D suspension cluster falling down¹⁴ and also presented briefly in ref.¹⁵ in the context of a jet. The rel-

ative simplicity of the model, focusing on the actual effect of long range hydrodynamic forces, allows to discuss the dominant physical features of the interface dynamics.

II. MODEL

We consider a system of N solid particles that move through an incompressible Newtonian fluid of viscosity η . The fluid is confined between two parallel plates separated at a distance $2d$ in the z direction, being infinite in the other two directions. To simplify the computation of the hydrodynamic interaction forces, and to focus on the effect of the long-range nature of them, we consider cylindrical particles of height L (slightly smaller than $2d$) and radius σ that have planar motion only. Particles are thin, i.e. $2d \ll \sigma$ and their mass is m .

The hydrodynamic forces between the cylinders in the confined geometry have been computed in Ref.¹⁴ in the Stokes regime for a dilute suspension. First, the force over the i -th particle has a drag component given by $-\frac{m}{\tau_1}\vec{u}_i$, where \vec{u}_i is the in-plane velocity of particle i and $\tau_1 = md/\pi\sigma^2\eta$ is the relaxation time of a single particle. Also, the presence of the other particles induce hydrodynamic forces over each other. When particles are far apart, the force on i due to the presence of k is

$$\vec{F}_{ik}^F = -\frac{m}{8\tau_1}\mathbb{K}(\vec{R}_{ki})\vec{u}_k \quad (1)$$

where $\vec{R}_{ki} = \vec{R}_i - \vec{R}_k$ is the relative distance between particles, being \vec{R}_i the position of the center of mass of the i -th particle and the tensor \mathbb{K} is given by

$$\mathbb{K}(\vec{R}) = (\sigma/R)^2(\mathbb{I} - 2\vec{R}\vec{R}/R^2) \quad (2)$$

This force depends both on the direction of the velocity \vec{u}_k and on the relative distance \vec{R}_{ik} . When \vec{u}_k is parallel to \vec{R}_{ik} , the interaction force on i is parallel to \vec{u}_k (drag), and if \vec{u}_k is perpendicular to \vec{R}_{ik} , the force turns out to be in an opposite direction to \vec{u}_k (antidrag).

On the other hand, when particles are close to each other, lubrication forces appear producing the net force on particle i due to the presence of k ¹⁴

$$\begin{aligned} \vec{F}_{ik}^N = & 2\pi d\eta \frac{1}{\sqrt{\epsilon}} \frac{1}{R_{ik}^2} \left(R_{ik}^2 \mathbb{I} - \vec{R}_{ik} \vec{R}_{ik} \right) \vec{u}_{ik} \\ & + \frac{3}{2} 2\pi d\eta \frac{d^2}{\sigma^2} \frac{1}{\epsilon} \frac{\vec{u}_{ik} \cdot \vec{R}_{ik}}{R_{ik}^2} \vec{R}_{ik} \end{aligned} \quad (3)$$

where $\epsilon = R_{ik}/\sigma - 1$ is the gap between the particles. The force depends on the relative velocities between the pair and it respects the action-reaction principle. Therefore it does not change the total momentum of the pair, but reduces the relative velocity.

The cutoff for using either expression (1) or (3) is rather arbitrary. We adopt the convention that when the pair is closer than R_{lubr} , the lubrication force (3) is used, when the distance is larger than R_{far} , the far force (1) is used, and in between a linear interpolation between the two is computed. The result is the interaction force \vec{F}_{ik}^I .

There is also an extra drag force produced by the flow between the particles and the plates¹⁴. This force can be added to the other drag force, simply modifying the prefactor by a value given by the particular experimental setup. In order to simplify the analysis, in what follows we will disregard the presence of this term but in case of being relevant to some experimental configuration, it can be trivially included.

In summary, the dynamical equations for the suspended particles are

$$m \frac{d\vec{u}_i}{dt} = -\frac{m}{\tau_1} \vec{u}_i + \sum_k \vec{F}_{ik}^I + m\vec{g} \quad (4)$$

that constitute a complex system of equations that will be solved numerically.

Although the tensor (2) diverges at close distances, it has the remarkable property that, its integral over the direction of \vec{R} vanishes. This implies that if a particle is surrounded by an homogeneous distribution of suspended particles, all moving with equal velocities, the far-field contribution to the hydrodynamic force vanishes.

The long range nature of the forces between particles makes it computationally expensive to perform direct numerical simulations where all pairs of forces are computed. However, the expressions (1) and (2) for the far-field contribution to the hydrodynamic forces, suggests that a mean field approximation can be done. In fact, if particles in a region move with similar velocities they exert similar forces to a target particle; it is natural then to group them altogether and compute the total force made by the group on any target particle. We define the coarse grained current \vec{J} on a cell c as

$$\vec{J}_c = \frac{1}{\Delta S} \sum_{i \in c} \vec{u}_i \quad (5)$$

where ΔS is the area of each cell.

Then, if the system is nearly homogeneous in each cell, the far field contribution to the force (1) can be approximated by

$$\vec{F}_i = -\frac{m}{8\tau_1} \sum_c \Delta S \mathbb{K}(\vec{R}_i - \vec{R}_c) \vec{J}_c \quad (6)$$

where the sum runs on all cells, \vec{R}_c is the position of the center of each cell. This expression allows to study systems of many particles at reasonable cost. Note that the vanishing integral of $\mathbb{K}(\vec{R})$ over the angles implies that (6) can be applied down to neighboring cells without producing divergences, but the mean field approximation can be inaccurate for near cells. Local inhomogeneities are not completely taken into account by the mean field and unrealistic vanishing forces can be obtained. To solve this problem, the mean field approximation of the far field force is applied only to cells that are separated by a distance larger than R_{mf} , otherwise the direct summation on the pair of particles is performed. Finally, the values chosen for performing the simulations are $R_{\text{lubr}} = 1.3\sigma$, $R_{\text{far}} = 2.0\sigma$, $R_{\text{mf}} = 5.66\sigma$. This numerical method was shown to give accurate results in the study of the spreading of a falling cluster¹⁴.

III. SIMULATIONS OF A FALLING JET

The long range forces (1) vanish when a particle is surrounded by and homogeneous medium, but in presence of inhomogeneities the force is finite. The effect of inhomogeneities is clearly seen when there a separation line between a region with suspended particles and a region without them; it was shown in¹⁴, that the force is enhanced if the separation line is curved, being possible to produce instabilities. As our description is for the dynamics of the suspended particles, and not for the surrounding fluid, it is sensible to call *free surface* the separation line between a region with suspended particles and the pure fluid.

In order to study the effect of the long range forces on the free surfaces and, in particular, if they can lead to unstable motion, we consider a falling jet of particles immersed in a fluid.

A jet of falling particles is studied numerically. Initially, a jet of $N = 24000$ particles is placed randomly at rest in a rectangle of width $L_x = 90\sigma$ and height $L_y = 600\sigma$. They fall down due to the action of a gravitational field pointing in the positive y direction. To mimic an infinity jet the vertical direction is periodic and the force computation uses the minimum image convention¹⁶. Units are chosen such that the particle diameter σ , particle mass m , and the relaxation time τ_1 are set to one. The gravitational force is $mg = 1.0$ and therefore the limiting velocity for a single particle $V_1^\infty = g\tau_1 = 1.0$ (see Eq. (4)).

Fig. 1 shows three successive snapshots of the jet. They show that the free surfaces become unstable, showing the appearance of waves. At the beginning the surface waves are characterized by short wavelengths but later as the amplitude of the perturbations growth, the characteristic wavelengths grow also. A coarsening process is developed leading to larger structures. Once the size of this structures is comparable to the

jet width, interactions between the two surfaces are observed and in-phase surface oscillations are obtained. The surface waves are also accompanied by modulations of the particle density.

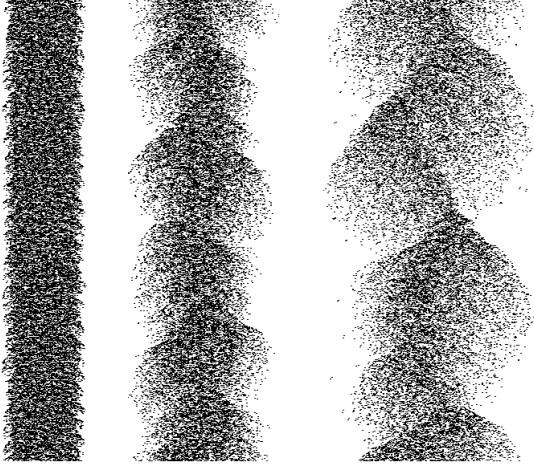


FIG. 1: Numerical simulation of a suspension of $N = 24000$ particles falling by the action of gravitational field. From the left to the right: $t = 200$, $t = 2000$, and $t = 4000$. Units are described in the text.

Fig. 2 shows the average vertical velocity of the falling jet as a function of time. It is seen that the jet rapidly gets an asymptotic velocity that is larger than the one for a single isolated particle. At much larger times, as the jet develops large structures and the particles separate, the falling velocity decreases and approaches $V_1^\infty = 1.0$.

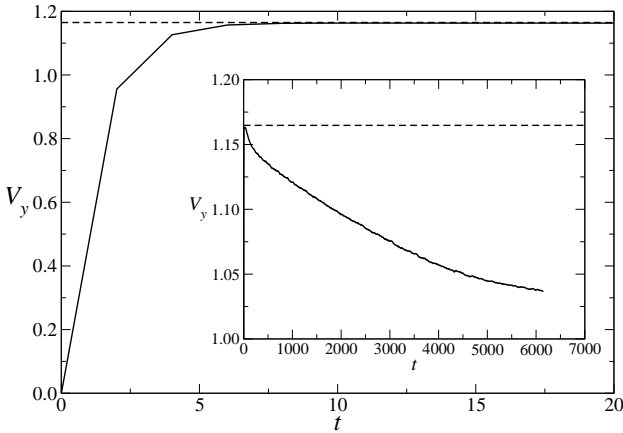


FIG. 2: Instantaneous average of the vertical velocity as a function of time (continuous line). The dashed line is the asymptotic theoretical value of the jet if it does not deform, $V_{\text{jet}}^\infty = 1.165$. Inset: evolution for longer times.

To describe in more detail the coarsening process, the x -integrated density $N_x(y, t)$ is studied, computed as the number of particles in a horizontal bin of height σ centered at y . In

Fig. 3 a spatio-temporal plot $N_x(y, t)$ is presented in the reference frame falling with the same instantaneous velocity of the jet. It is seen that structures grow in time showing the coarsening process. Also, the structures propagate in the negative y direction; as the plot is presented in the reference frame of the falling jet it indicates that the perturbations fall at a slightly smaller velocity than the jet.



FIG. 3: Spatiotemporal diagram of the evolution of the x -integrated density $N_x(y, t)$ in the reference frame of the falling jet. Time is on the vertical axis and increasing upward. The horizontal axis is the y coordinate, with periodic boundary conditions, and the gravitational acceleration points to the right. The gray scale is proportional to density, with lighter regions representing denser regions of the system, the minimum and maximum represented densities are $N_x^{\min} = 11$ and $N_x^{\max} = 82$, respectively, and the average is $N_x^{\text{avg}} = N/L_y = 40$. The simulation parameters are the same as in Fig. 1 and the total simulation time is $t = 6152$.

IV. GLOBAL MODEL

The behavior observed in the numerical simulations suggest an instability like the observed when two immiscible fluids in contact move with a relative velocity (Kelvin-Helmholtz instability)¹⁷.

To describe the appearance of the surface instability, we build a global model, similar to hydrodynamic equations. We consider the particle number density $n(\vec{R})$ and the particle mean velocity $\vec{V}(\vec{R})$. The average force density over the suspension, produced by the drag force, the far force contribution (1), and the gravity acceleration is

$$\vec{F}(\vec{R}) = -\frac{1}{\tau_1}\vec{J}(\vec{R}) - \frac{1}{8\tau_1}n(\vec{R}) \int d\vec{R}' \mathbb{K}(\vec{R} - \vec{R}')\vec{J}(\vec{R}') + n(\vec{R})m\vec{g} \quad (7)$$

with $\vec{J} = mn\vec{V}$ is the mass current density.

In a Euler-like global model as the one proposed, the lubrication force contribution can be neglected because its effect

is to reduce velocity fluctuations, but it does not modify the mean velocity as it only affects the relative velocity. Eventually, its effect would be to produce an additional effective viscosity as obtained in kinetic theory¹⁸.

Therefore a global equation of motion for the suspension can be written as

$$\frac{\partial n}{\partial t} + \nabla \cdot (n \vec{V}) = 0 \quad (8)$$

$$nm \left(\frac{\partial \vec{V}}{\partial t} + \vec{V} \cdot \nabla \vec{V} \right) = \vec{F} \quad (9)$$

Before analyzing the development of the instabilities, let's consider the evolution of a unperturbed homogeneous jet. For a thin jet of width L_x and height L_y , with periodic boundary conditions in y , if the particle current is assumed to be homogeneous $\vec{J}(\vec{R}, t) = J_{\text{jet}}(t) \hat{y}$, the integral term in (7) simplifies (see Eq. (A2)) and we have that

$$\int d\vec{R}' \mathbf{K}(\vec{R} - \vec{R}') \vec{J}_{\text{jet}} = 2\sigma^2 \left[\arctan(L_y/L_x) - \arctan(L_x/L_y) \right] J_{\text{jet}} \hat{y} \quad (10)$$

independent of \vec{R} . Therefore Eqs. (8) and (9) admit a solution of an homogeneous falling jet with velocity

$$V_{\text{jet}}(t) = g\tau_{\text{jet}} \left(1 - e^{-t/\tau_{\text{jet}}} \right) \quad (11)$$

where the jet relaxation time is

$$\tau_{\text{jet}} = \frac{\tau_1}{1 - n_0 \sigma^2 \left[\arctan(L_y/L_x) - \arctan(L_x/L_y) \right] / 4} \quad (12)$$

and n_0 is the jet number density.

Note that the asymptotic velocity as the relaxation time is different from the one of a single falling particle $V_1^\infty = g\tau_1$. This effect is due to the long range hydrodynamic interactions. A peculiar feature is that the modification of the falling velocity depends only on the system shape, but not on its size. A similar phenomena was observed in the case of a falling circular cluster¹⁴. In fact, for a thin jet ($L_x < L_y$) most of the relative distances between particles are parallel to the falling velocity, giving rise to a positive hydrodynamic forces between particles. That is particles exerts a positive drag, in the direction of the motion, increasing the falling velocity. On the other hand, if the jet were wide ($L_x > L_y$) most of the relative distances between particles would be perpendicular to the falling velocity and the dominant contribution of the hydrodynamic forces would be the antidrag, reducing the jet falling velocity. In the case of the jet we are considering the theoretical values for the falling jet velocity and relaxation time are $V_{\text{jet}}^\infty = 1.165$ and $\tau_{\text{jet}} = 1.165$, that are larger than the values for a single particle. In Fig. 2 it is seen that the jet rapidly gets this velocity and afterward, when it starts deforming, the velocity slowly decreases approaching $V_1^\infty = 1.0$. This long time value is consistent with Eqs. (11) and (12), when the jet density decreases. An exponential fit to the early time evolution of the velocity of the jet gives the same relaxation time as predicted.

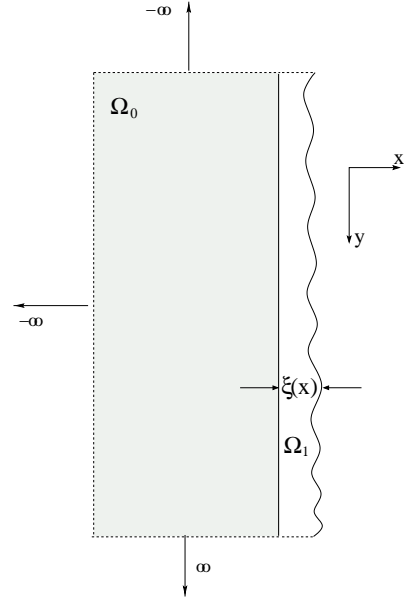


FIG. 4: Left: Sketch of the semi - infinity suspension. Ω_0 is the unperturbed domain, Ω_1 is the perturbed domain, ξ is the perturbation in the x direction.

In presence of a free surface, an additional equation must be added to describe the evolution of the free surface position $\xi(y, t)$ (see Fig. 4). The mean suspension velocity at the surface must be equal to the surface velocity¹⁷.

$$\frac{\partial \xi}{\partial t} + V_y \Big|_{x=\xi} \frac{\partial \xi}{\partial y} = V_x \Big|_{x=\xi} \quad (13)$$

V. LINEAR STABILITY ANALYSIS

The stability of the free surface of the jet is analyzed using the global Eqs. (8), (9), and (13). To simplify the problem and assuming that at the beginning the two free surfaces do not interact strongly, we will consider the simpler case of a single free surface, limiting a semi-infinite homogeneous suspension in the $x < 0$ region, of density n_0 . In this geometry the jet falling velocity is $\vec{V}_0 = g\tau_1 \hat{y} / (1 + \beta_0/4)$, where $\beta_0 = \pi \sigma^2 n_0 / 4$ is the area fraction of the suspension (see Eq. (A3)). Note that in this geometry $V_0 < V_1^\infty$.

We consider small perturbations of the free surface. Introducing a formal parameter $\epsilon \ll 1$, the fields are written as $\vec{V}(\vec{R}) = \vec{V}_0 + \epsilon \vec{V}_1(\vec{R})$, $n = n_0 + \epsilon n_1(\vec{R})$, and $\xi = \epsilon \xi_1(y)$. The domain Ω over which the integration in (7) must be done can be split into the initial domain $\Omega_0 : x \leq 0$, plus a perturbed domain $\Omega_1 : 0 < x \leq \xi(y, t)$ (see Fig. 4). Keeping terms up to

linear order in ϵ , the equations read

$$\frac{\partial n_1}{\partial t} + n_0 \nabla \cdot \vec{V}_1 = 0 \quad (14)$$

$$\begin{aligned} \frac{\partial \vec{V}_1}{\partial t} + \vec{V}_0 \cdot \nabla \vec{V}_1 = & -\frac{1}{\tau_1} \vec{V}_1(\vec{R}) - \frac{1}{2\tau_1} \frac{n_1}{4} \mathbb{K}(\hat{y}) \vec{J}_0 \\ & - \frac{1}{2\tau_1} n_0 \int_{\Omega_0} d\vec{R}' \mathbb{K}(\vec{R} - \vec{R}') \vec{J}_1(\vec{R}') \\ & - \frac{1}{2\tau_1} n_0 \int_{-\infty}^{\infty} dy' \mathbb{K}(\vec{R} - y' \hat{y}) \vec{J}_0 \xi(y') \end{aligned} \quad (15)$$

$$\frac{\partial \xi}{\partial t} + V_{0y} \Big|_{x=0} \frac{\partial \xi}{\partial y} = V_{1x} \Big|_{x=0} \quad (16)$$

The deformed surface has a long range effect of the fluid motion, as reflected by the last term in Eq. 15.

This integro-differential system of equations does not have an evident analytic solution. However, an estimation of the instability modes can be obtained as follows. A Fourier expansion of the fields $A_1(\vec{R}, t) = \hat{A}_1(\vec{k}, t) e^{i\vec{k} \cdot \vec{R}}$ is performed. As the Fourier basis is not a solution of the system (particularly because of the integral terms in (15)), we obtain an estimation by evaluating the equations at $x = 0$. Defining dimensionless variables $\rho = \hat{n}_1/n_0$, $\vec{U} = \vec{V}_1/(g\tau_1)$, $\varphi = \xi/(g\tau_1^2)$, $\vec{q} = (g\tau_1^2)\vec{k}$, and $s = t/\tau_1$, the equations read

$$\frac{\partial \rho}{\partial s} = -i\vec{q} \cdot \vec{U} - i\vec{q} \cdot \vec{U}_0 \rho \quad (17)$$

$$\frac{\partial \vec{U}}{\partial s} = -\vec{U} - i(\vec{q} \cdot \vec{U}_0) \vec{U} - \mathbf{Q}_1(\vec{U} + \rho \vec{U}_0) - \mathbf{Q}_2 \vec{U}_0 \varphi \quad (18)$$

$$\frac{\partial \varphi}{\partial s} = U_x - i(\vec{q} \cdot \vec{U}_0) \varphi \quad (19)$$

with the following defined tensors (see Eq. (A5))

$$\mathbf{Q}_1 = \frac{\beta_0}{2} \left\{ \begin{pmatrix} 1 & 0 \\ 0 & -1 \end{pmatrix} + \frac{|q_y|}{iq_x + |q_y|} \begin{pmatrix} -1 & i \\ i & 1 \end{pmatrix} \right\} \quad (20)$$

$$\mathbf{Q}_2 = \frac{\beta_0}{2} |q_y| \begin{pmatrix} -1 & i \\ i & 1 \end{pmatrix} \quad (21)$$

We recall the the dimensionless jet falling velocity is $\vec{U}_0 = \hat{y}/(1 + \beta_0/4)$

The tensors \mathbf{Q}_1 and \mathbf{Q}_2 capture the effect of the long range forces produced by the perturbations, when they are integrated in the semi-infinite volume. \mathbf{Q}_1 describes the interaction of the perturbations with the bulk and \mathbf{Q}_2 the interaction with the free surface. Remarkably, \mathbf{Q}_2 is proportional to q and not to q^2 , therefore the effect of a curved surface cannot be described in terms of a surface tension. Note also that \mathbf{Q}_1 is independent of the magnitude of \vec{q} and depends only on its direction. This fact has an important consequence because in the limit of perturbations of small wave vectors the effect of the hydrodynamic interactions does not vanish. In fact in the limit $q \rightarrow 0$ the linear system of equations (19) has a Jordan-block structure and admits a solution of the form (at first order in β_0)

$$\rho = 2AU_0^{-1}(-\cos \phi + i|\sin \phi|) \quad (22)$$

$$U_x = A\beta_0|\sin \phi| \quad (23)$$

$$U_y = -A\beta_0 \cos \phi \quad (24)$$

$$\varphi = A\beta_0|\sin \phi|t \quad (25)$$

where A is an arbitrary coefficient given by the initial condition and ϕ is the angle between the wave vector \vec{q} and the \hat{x} direction. The solution shows a linear, instead of exponential, increase in time of the surface oscillations.

For larger values of q the system of equations looses its Jordan-block structure and solutions in the form $\exp(\lambda s)$ are looked for. The eigenvalues λ for $q \ll 1$, $\beta_0 \ll 1$, and $0 < \phi < \pi$ ($\sin \phi > 0$) are

$$\lambda_1 = -iU_0q(1 + \beta_0/4) \sin \phi + \frac{\sqrt{3}}{4}\beta_0U_0q \sin \phi + O(q^2) \quad (26)$$

$$\lambda_2 = -iU_0q(1 + \beta_0/4) \sin \phi - \frac{\sqrt{3}}{4}\beta_0U_0q \sin \phi + O(q^2) \quad (27)$$

$$\lambda_3 = -1 - \frac{\beta_0}{2}(\cos \phi + i \sin \phi) + O(q) \quad (28)$$

$$\lambda_4 = -1 + \frac{\beta_0}{2}(\cos \phi + i \sin \phi) + O(q) \quad (29)$$

and similar results for $\pi < \phi < 2\pi$ ($\sin \phi < 0$).

Two of the eigenvalues, λ_3 and λ_4 have negative real parts for small q and therefore correspond to damped motion. However, the real part of λ_1 (λ_2 for $\pi < \phi < 2\pi$) is positive. Therefore an instability is predicted. The analysis shows that the system becomes unstable for any strength of the gravitational force and, coming back to the original units, the instability rate is directly proportional to V_0k . In the limit $k \ll 1$ the real parts of λ_1 and λ_2 are proportional to the wavevector. It is reasonable to expect that a more detailed model, that includes terms proportional to gradients of \vec{V} or the viscous effect due to the lubrication forces, will produce that for high enough wave vectors, the real part of the eigenvalues become negative again. Hence, it is expected that the system is unstable for a range of wave vectors going from zero to a finite value, showing the coarsening process observed in the simulation¹⁹.

The eigenvalues λ_1 and λ_2 have also an imaginary part. The dominant one with respect to k and β_0 is $\lambda_{1I} = -iqU_0(1 + \beta_0/4) \sin \phi$. It corresponds to a wave in the form $\exp(iq \sin \phi(y - U_0(1 + \beta_0/4)t) + iq \cos \phi x)$, that propagates in the $+y$ direction, with phase velocity $U_0(1 + \beta_0/4) = 1$. That is, the structures propagate at the same velocity than a single falling particle. This phase velocity is larger than the jet falling velocity by a factor $O(\beta_0)$. As a consequence, the unstable structures should move faster than the jet. In the simulations, we actually find the opposite: the structures move slower than the jet. This change of character can be due to the different geometries as they are considered, as it also happens to the jet falling velocity that in one case is faster than V_1^∞ , while in the other case was found slower.

The linear stability analysis for a jet with two free surfaces as in the simulations is much more involved. One extra equation must be added and the long range interactions in this geometry give more complex expressions, as can be seen in the

case of the falling velocity. Nevertheless, we expect that the analysis presented here, showing that the surface is unconditionally unstable and the growth rates are proportional to the wave vectors, is preserved.

We have studied numerically the growth rate for different wavevectors in the jet. For each wavevector we have performed new simulations, with an initial condition similar to the one described previously for the jet except that the x coordinates are modulated in such a way to create two waves of vectors $k_y = 2\pi n_y/L_y$ in the surface positions. In practice we map the initial x coordinates of the original rectangular jet as $[0, L_x] \rightarrow [-A \cos(k_y y), L_x + A \cos(k_y y)]$. In each simulation we compute the evolution of the Fourier amplitudes $\Psi_n = N^{-1} |\sum_i (x_i - L_x/2)^2 e^{2\pi i n_y y_i / L_y}| = N^{-1} |\int \rho(x, y) (x - L_x/2)^2 e^{2\pi i n_y y / L_y}|$, with the same wavenumber as the perturbation. These Fourier amplitudes measure, at linear order, the amplitude of $\xi(k_y)$. Fig. 5 shows the results of the Fourier amplitudes for the simulations done with $n_y = 1, 2, 3, 4$. For $n_y = 1$ a linear increase of Ψ is observed while for $n_y \geq 2$ exponential increase of the Ψ 's are obtained, until nonlinear interaction between modes appear. The growth rates are $\lambda(n_y = 2) = 1.21 \times 10^{-3}$, $\lambda(n_y = 3) = 1.82 \times 10^{-3}$, and $\lambda(n_y = 4) = 2.19 \times 10^{-3}$, that are roughly in the ratio 2 : 3 : 4, confirming the linear proportionality with k . However, no direct comparison with the prediction can be made because only k_y was fixed but not k_x , therefore the angle ϕ takes all possible values. Larger values of n_y give very noisy results to be

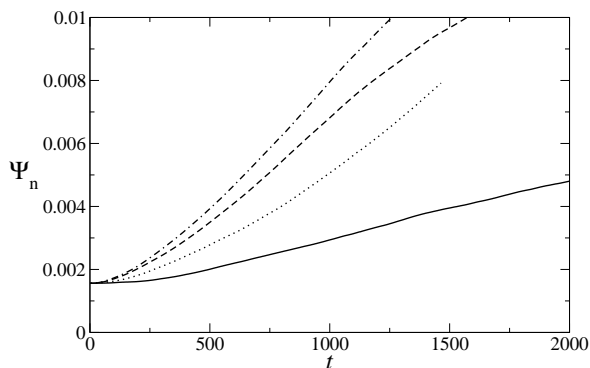


FIG. 5: Evolution of the Fourier amplitudes Ψ_n computed with the same wavenumber n as the perturbation made on the surface. $n = 1$ continuous line, $n = 2$ dotted line, $n = 3$ dashed line, and $n = 4$ dash-dotted lined.

VI. CONCLUSIONS

In conclusion, we investigated the dynamical evolution, in the Stokes regime, of a jet of falling particles confined in an Hele-Shaw cell. The free surfaces of the jet is shown to become unstable and a coarsening process takes place from the smallest sizes up to the largest structures.

A continuous Euler-like hydrodynamic model for the suspension is presented which describes the main features of the jet flow. In particular, the model predicts a geometry dependent falling velocity for the jet (thin jets fall slower than thick jets).

The theoretical analysis shows that the free surface is unstable to any gravitational force and any wave vector. The growth rates are proportional to the wave vectors, result that is consistent with the coarsening process observed in the simulations. Finally, the model predicts that the structures move with a velocity slightly different than the jet's velocity, as observed in the simulations but with a different sign prediction. In this problem we find that the interface dynamics is quite different than the usual immiscible fluid case where the surface tension play a leading role such as to select and stabilize structures. For the present jet, the particle hydrodynamic interactions create a surface instability essentially due to long range effects caused by flow recirculation around a particle. A crucial point is that this effect is scale free. We observe at the end of the simulations a partial mixing due to flow structuration as well as hydrodynamic dispersion causing a diffuse interface.

Finally, we open a question on the relation between this model and the dynamics of actual non-Brownian suspensions in a confined cell. Though we have here a situation a little bit artificial as the problem is solved in the case of particle sizes (diameter) larger than the cell gap, we believe that all the features dealing with scales larger than the gap (essentially the long range interactions) will survive at the qualitative level.

Acknowledgments

The authors thank P. Cordero and M. Malek Mansour for their comments. A. Alvarez and R. Soto. are grateful with the hospitality of CECAM, ENS-Lyon where part of this work was done. The simulations were done in the CIMAT's parallel cluster. This work has been partly financed by the *Fondcyt* research grant 1030993, the ECOS-Conicyt research grant C03E05 and the *Fondap* grant 11980002. A.A. acknowledges the financial support of a *Mecesup* grant.

* Electronic address: rsoto@dfi.uchile.cl

¹ J. Happel and H. Brenner, "Low Reynolds Number Hydrodynamics, with Special Applications to Particulate Media" Prentice-Hall, London, 1965.

² J.F. Brady and G. Bossis, "Stokesian dynamics", Annu. Rev. Fluid. Mech. **20**, 111 (1988).

³ A. J. C. Ladd, "Effect of container walls on the velocity fluctua-

tions of sedimenting spheres" Phys. Rev. Lett. **88**, 048301 (2002).

⁴ S. Kim and S. J. Karrila, *Microhydrodynamics: Principles and Selected Applications* Butterworth-Heinemann Series in Chemical Engineering, Stoneham 1991.

⁵ H.A.Stone, A.D.Stroock and A.Ajdari, "Engineering flows in small devices : Microfluidics towards a lab-on-chip", Annu. Rev. Fluid. Mech. **20**, 111 (2004).

- ⁶ B.H.Weigl and P. Yager, “Microfluidic diffusion-based separation and detection”, *Science* **283**, 346 (1999).
- ⁷ F. Rouyer, J. Martin, and D. Salin, “Structure, density, and velocity fluctuations in quasi-twodimensional non-Brownian suspensions of spheres”, *Phys. Rev. Lett.* **83**, 1058 (1999).
- ⁸ J. Santana-Solano and J. Arauz-Lara, “Hydrodynamic interactions in quasi-two-dimensional colloidal suspensions”, *Phys. Rev. Lett.* **87**, 038302 (2001).
- ⁹ B. Cui et al., “Anomalous hydrodynamic interaction in a quasi-twodimensional suspension” *Phys. Rev. Lett.* **92**, 258301 (2004).
- ¹⁰ P. Petitjeans, C.Y. Chen, E. Meiburg, T. Maxworthy “Miscible quarter five-spot displacements in a Hele-Shaw cell and the role of flow-induced dispersion” *Phys. Fluids*, **11**1705 (1999).
- ¹¹ J. M. Nitsche and G. K. Batchelor, “Break-up of a falling drop containing dispersed particles”, *J. Fluid Mech.*, **340**, 161 (1997).
- ¹² G. Machu, W. Meile, L. C. Nitsche and U. Schafflinger, “Coalescence, torus formation and breakup of sedimenting drops: experiments and computer simulations”, *J. Fluid Mech.*, **447**, 299 (2001).
- ¹³ Maxime Nicolas, *Phys. Fluids* **14**, “Experimental study of a gravity driven dens suspension jet” *Phys. of Fluids* **14**, 3570 (2002).
- ¹⁴ A. Alvarez and R. Soto, *Phys. of Fluids* “Dynamics of a suspension confined in a thin cell” *Phys. of Fluids* **17**, 093103 (2005).
- ¹⁵ A. Alvarez R. Soto and E.Clement, “Free surface instability in a confined suspension jet”, *Physica A* **356**, 196 (2005).
- ¹⁶ M. P. Allen y D. J. Tildesley, *Computer Simulation of Liquids* (Oxford Science Publications, New York, 1990).
- ¹⁷ S. Chandrasekhar, *Hydrodynamic and Hydromagnetic Stability*. International Series of Monographs on Physics, Dover, Oxford 1981.
- ¹⁸ S. Chapman and T. G. Cowling, *The Mathematical Theory of Non-Uniform Gases*, third edition. Cambridge University Press, New York, 1970.
- ¹⁹ P. Politi and C. Misbah, “When Does Coarsening Occur in the Dynamics of One-Dimensional Fronts?” *Phys. Rev. Lett.* **92**, 090601 (2004)

APPENDIX A: KERNEL INTEGRALS

Some integrals of the kernel $\mathbb{K}(\vec{R})$ (2) used in the manuscript are:

(a) Homogenous integral for the jet

$$\begin{aligned}
 I_1 &= \int_{-L_x}^{L_x} dx' \int_{-L_y}^{L_y} dy' \mathbb{K}(\vec{R} - \vec{R}') \\
 &= 2\sigma^2 \left[\arctan\left(\frac{L_y}{L_x - x}\right) - \arctan\left(\frac{L_x + x}{L_y}\right) \right] \begin{pmatrix} 1 & 0 \\ 0 & -1 \end{pmatrix} \quad (\text{A1})
 \end{aligned}$$

where $\vec{R} = x\hat{x} + y\hat{y}$ is any vector in the interior of the integration domain and we have used periodic boundary conditions in y . When $L_y \gg L_x$ the integral depends slightly on x and its horizontal average is in that limit

$$I_1 \approx 2\sigma^2 \left[\arctan(L_y/L_x) - \arctan(L_x/L_y) \right] \begin{pmatrix} 1 & 0 \\ 0 & -1 \end{pmatrix} \quad (\text{A2})$$

(b) Homogenous integral for the semiinfinite system

$$I_2 = \int_{-\infty}^0 dx' \int_{-\infty}^{\infty} dy' \mathbb{K}(\vec{R} - \vec{R}') = -\frac{\pi\sigma^2}{2} \begin{pmatrix} 1 & 0 \\ 0 & -1 \end{pmatrix} \quad (\text{A3})$$

with $\vec{R} = x\hat{x} + y\hat{y}$ any vector with $x < 0$ and we have used periodic boundary conditions in y .

(c) Fourier transform for the semiinfinite system

$$\begin{aligned}
 I_3 &= \int_{-\infty}^0 dx' \int_{-\infty}^{\infty} dy' \mathbb{K}(\vec{R} - \vec{R}') e^{i\vec{k} \cdot \vec{R}'} \\
 &= \pi\sigma^2 \left[\begin{pmatrix} 1 & 0 \\ 0 & -1 \end{pmatrix} - \frac{|k_y|}{ik_x + |k_y|} \begin{pmatrix} 1 & -i \\ -i & -1 \end{pmatrix} \right] \quad (\text{A4})
 \end{aligned}$$

with $\vec{R} = x\hat{x} + y\hat{y}$ any vector with $x < 0$ and we have used periodic boundary conditions in y .

(d) Fourier transform for the interface line

$$\begin{aligned}
 I_4 &= \int_{-\infty}^{\infty} dy \mathbb{K}(x\hat{x} + y\hat{y}) e^{iky} \\
 &= \pi\sigma^2 \left\{ \delta(x) \begin{pmatrix} 1 & 0 \\ 0 & -1 \end{pmatrix} - |k| e^{-|kx|} \begin{pmatrix} 1 & -i \\ -i & -1 \end{pmatrix} \right\} \quad (\text{A5})
 \end{aligned}$$

The Dirac delta appears when \mathbb{K} is evaluated up to the origin, that physically cannot happen because the interaction is replaced by the lubrications forces. Therefore, this term will be eliminated in the evaluation of the kernel integrals.